

# THE EARTH'S MAGNETIC FIELD AND ITS DYNAMO ORIGIN

BINOD SREENIVASAN\*

---

*The Earth's magnetic field is powered by convection occurring in its fluid outer core. Variations in the intensity of core convection over geological time are believed to cause the highly dynamic behaviour of the geomagnetic field, which includes excursions and occasional polarity reversals. Although numerical models of the geodynamo operate in regimes far from that in the Earth's core, they reproduce the dipole-dominated structure of the field in a large region of the parameter space as well as reversals in strongly driven convection.*

---

## Introduction

It has been known for centuries that the Earth has a large-scale magnetic field of internal origin. The earliest discoveries related to geomagnetism are credited to the Chinese, who used compasses made of lodestone for navigation. Gilbert, in his treatise *De Magnete* (1600), proposed that the force acting on a compass needle originated within the Earth. Subsequently, navigators measured the angle between the magnetic north and true north - known as the magnetic declination - to conclude that the Earth's field was in fact slowly changing with time. Halley<sup>1,2</sup> observed a systematic westward drift of the field, which he attributed to the slightly slower rotation of the planet's solid core relative to its crust, a hypothesis that relied on the assumption that the core was uniformly magnetized. However, it was later evident that the permanent magnetism of ferromagnetic materials cannot be sustained above the Curie temperature, so the Earth's field must have its origins in electric currents induced within the core. Through his famous disk dynamo, Faraday showed that an electrical conductor moving in a static magnetic field produces an electric current. If a disk dynamo operates such that the induced electric current flows through a loop in the same direction as the sense of spin<sup>3</sup>, an induced magnetic field forms that reinforces the pre-existing field. In 1919, Larmor<sup>4</sup> proposed that motions of an electrically

conducting fluid could sustain the magnetic fields in sunspots. Earlier studies in seismology<sup>5,6</sup> had led to the inference that the Earth's outer core is liquid because of its inability to transmit shear waves. Hence Larmor's idea of a *fluid dynamo* was an attractive proposition for the Earth and many other planetary bodies. If there were no fluid motions in the Earth's core, an initial magnetic field would have decayed away by ohmic diffusion on a timescale of  $\sim 10^4$  years<sup>3</sup>. Yet, the Earth has had a magnetic field for at least 3 billion years<sup>7</sup>, which can be explained by a process of field generation through induction in its core.

Fluid motion in present day Earth's core is thought to be driven by thermo-chemical convection. Buoyant blobs of light elements released from the boundary of the inner core constantly stir the fluid outer core, apart from bulk motion arising from temperature differences. Current estimates of the age of the inner core are less than 1 Gyr<sup>8</sup>. It is therefore likely that the Earth's dynamo has operated in its early stages, that is, before inner core nucleation, on purely thermal convection caused by gradual cooling. The geodynamo problem requires solution of the magnetohydrodynamic (MHD) equations, which simultaneously determine the magnetic field, velocity and temperature (or composition) in a conducting fluid confined between two spherical surfaces. Considerable progress has been made in modelling convection in rotating spherical shells and their consequences for dynamo action<sup>9,10</sup>. In particular, dynamo models have been successful in

---

\* Centre for Earth Sciences, Indian Institute of Science, Bangalore 560 012, India. e-mail : bsreeni@iisc.ac.in

reproducing two key features of the geomagnetic field – its large-scale dipole-dominated structure and occasional polarity reversals. This paper summarizes some of the influential developments in geodynamo theory.

### A Brief History of Geodynamo Theory

Elsasser<sup>11</sup> initiated the study of the interaction between three-dimensional velocity and magnetic fields in the context of the Earth's core. He suggested decomposing the two fields into poloidal and toroidal components and then expanding them in spherical harmonics. This approach was developed further by Bullard & Gellman<sup>12</sup> and is being used in many dynamo models. For example,

$$\mathbf{u} = \nabla \times (T \hat{\mathbf{r}}) + \nabla \times \nabla \times (P \hat{\mathbf{r}}); \quad (1)$$

$$T(r, \theta, \phi, t) = \sum_{l=0}^L \sum_{m=-1}^l T_l^m(r, t) Y_l^m(\theta, \phi) \quad (2)$$

where  $T$  and  $P$  are the toroidal and poloidal components of  $\mathbf{u}$ ,  $\hat{\mathbf{r}}$  is the unit vector in the radial direction and  $Y_l^m$  is a normalized spherical harmonic function.

Bullard & Gellman outlined a cyclic process by which a poloidal magnetic field can regenerate itself. A toroidal field is swept out from an existing poloidal field through differential rotation (figure 1a); and a helical motion comprising an upwelling and a twist recreates a poloidal field from a toroidal field (figure 1b). These two events are popularly known as the  $\Omega$ -effect and the  $\alpha$ -effect respectively. Parker<sup>13</sup> independently developed the theory

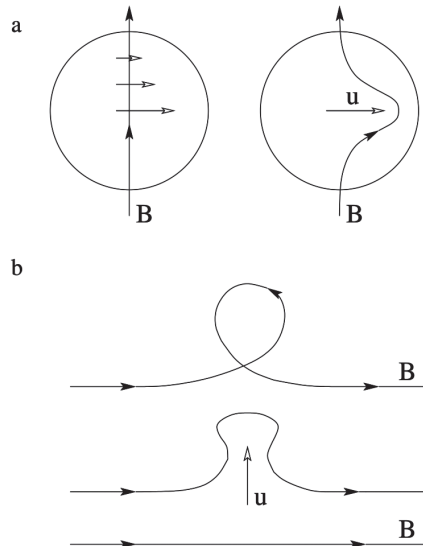


**Figure 1:** Schematic of the  $\alpha$ - $\Omega$  dynamo cycle.<sup>3,12</sup> (a) An initial poloidal field is swept by differential rotation to produce a toroidal field; and (b) an upwelling lifts and twists a toroidal field line to produce a poloidal field loop. (Figure adapted from Sreenivasan, Curr. Sci. (2010), 99, 1739–1750).<sup>15</sup>

of dynamos based on the  $\Omega$  and  $\alpha$  effects and suggested that the helical motion that produces the poloidal field can happen in cyclonic and anticyclonic vortices. Steenbeck *et al.*<sup>14</sup> provided a mathematical framework for the  $\alpha$ -effect by noting that a small-scale, non-axisymmetric velocity  $\mathbf{u}'$  interacts with a small-scale magnetic field  $\mathbf{b}'$  to generate a large-scale electromotive force  $\bar{\mathbf{E}} = \overline{\mathbf{u}' \times \mathbf{b}'}$ , which, in turn, is proportional to the mean magnetic field  $\mathbf{B}_0$ . (The constant of proportionality here is commonly denoted by  $\alpha$ .)

The kinematic dynamo problem<sup>16,17</sup> addresses the question of whether or not a given flow  $\mathbf{u}$  can generate a magnetic field  $\mathbf{B}$ . The magnetic field is governed by Maxwell's equations and Ohm's law for a moving conductor<sup>18</sup>. Combining these gives the magnetic induction equation, which determines the evolution of  $\mathbf{B}$ :

$$\frac{\partial \mathbf{B}}{\partial t} = \nabla \times (\mathbf{u} \times \mathbf{B}) + \eta \nabla^2 \mathbf{B}. \quad (3)$$

Here,  $\eta$  is the magnetic diffusivity, which is related to the magnetic permeability  $\mu$  and the electrical conductivity  $\sigma$  by  $\eta = (\mu\sigma)^{-1}$ . Magnetic field growth happens when convection of  $\mathbf{B}$ , given by the first term on the right-hand side of equation (3), exceeds magnetic diffusion, given by the second term. The ratio of the two terms gives the magnetic Reynolds number,  $R_m = u_* L / \eta$ , where  $u_*$  is the characteristic velocity and  $L$  is the length scale.

Although kinematic dynamos tell us which flows can produce growth of the magnetic field, they do not consider the back-reaction of the magnetic field on the velocity. To ensure the coupled evolution of  $\mathbf{u}$  and  $\mathbf{B}$ , the induction equation (3) must be solved in conjunction with the momentum equation for an electrically conducting fluid. Furthermore, if the fluid motion is driven by thermal convection, then the temperature must also be solved for. We then have the additional equations,

$$\begin{aligned} \frac{\partial \mathbf{u}}{\partial t} + (\mathbf{u} \cdot \nabla) \mathbf{u} + 2\Omega \times \mathbf{u} \\ = -\frac{1}{\rho_0} \nabla p - \frac{\rho}{\rho_0} g + \frac{1}{\rho_0} \mathbf{j} \times \mathbf{B} + \nu \nabla^2 \mathbf{u}, \end{aligned} \quad (4)$$

$$\frac{\partial T}{\partial t} + (\mathbf{u} \cdot \nabla) T = \kappa \nabla^2 T + Q_s, \quad (5)$$

where  $\mathbf{u}$  and  $\mathbf{B}$  also satisfy the divergence-free conditions.

$$\nabla \cdot \mathbf{u} = 0; \quad \nabla \cdot \mathbf{B} = 0. \quad (6)$$

The terms on the left-hand side of equation (4) represent linear and nonlinear inertia (which together give the material derivative  $D\mathbf{u}/Dt$ ), and the Coriolis force. The forces on the right-hand side are, in their order of appearance, the fluid pressure modified by centrifugal acceleration, buoyancy, magnetic (Lorentz) force and viscous diffusion. In the above equations  $\boldsymbol{\Omega}$  is the background rotation vector that points in the z-direction,  $\mathbf{g}$  is the local gravitational acceleration,  $\rho$  and  $\rho_0$  are the local and far-field densities,  $\kappa$  is the thermal diffusivity and  $Q_s$  is a uniform volumetric heat source/sink.

In geodynamo models, equations (3)–(6) are made dimensionless and solved numerically for an incompressible fluid confined between two concentric spherical surfaces that mimic the Earth's inner core boundary (ICB) and the core–mantle boundary (CMB). The code usually employs spherical harmonic expansions in the angular coordinates  $(\theta, \phi)$ , whereas the radial coordinate  $r$  may be discretized using finite differences or by a Chebyshev polynomial. The numerical method and boundary conditions can be found in several papers.<sup>19,20,21</sup>

The dimensionless parameters of interest in the geodynamo problem are the Ekman number, the Rayleigh number, the Prandtl number, the magnetic Prandtl number. (The magnetic Reynolds number is an intrinsic parameter.) The Ekman number,  $E = v/2\Omega L^2$ , is the ratio of the viscous to Coriolis forces and is  $\sim 10^{-15}$  for the core. However, some studies replace the molecular value of the viscosity  $v$  by a *turbulent* viscosity  $v_T$  and propose  $E \sim 10^{-9}$ . The Rayleigh number for convection can have different definitions depending on the mode of heating. For differential heating driven by a temperature difference  $\Delta T$ ,  $Ra = g\beta\Delta TL^3/v\kappa$ , where  $L$  is the gap-width of the spherical shell,  $\beta$  is the coefficient of thermal expansion and  $\kappa$  is the thermal diffusivity. (The thermal diffusivity is related to the thermal conductivity  $\kappa$ , specific heat capacity at constant pressure  $c_p$  and density  $\rho$  by  $\kappa = k/\rho c_p$ .) In dynamo models the classical Rayleigh number is often multiplied by the Ekman number to give a ‘modified’ Rayleigh number<sup>19</sup>,  $Ra_M = g\beta\Delta TL/2\Omega\kappa$ . Estimates for  $Ra$  in the core vary from approximately the critical value for onset of convection<sup>22</sup>,  $Ra_c$  to several orders of magnitude above  $Ra_c$ <sup>23,24</sup>, even if the turbulent value of the diffusivity  $\kappa_T$  is adopted in place of its molecular value. The Prandtl number,  $Pr$  is given by  $v/\kappa$  and the magnetic Prandtl number,  $Pm$  is  $v/\eta$ . The Roberts number, given by  $q = PmPr^{-1} = \kappa/\eta$ , is a popular dimensionless group in many models, with a molecular value of  $\sim 10^{-6}$  and a turbulent value of order unity<sup>24</sup>.

Present day numerical geodynamo models mostly operate in the regime  $E \gtrsim 10^{-7}$ ,  $q = \kappa/\eta \gtrsim 0.05$  and  $Ra/Ra_c \lesssim 100$ .

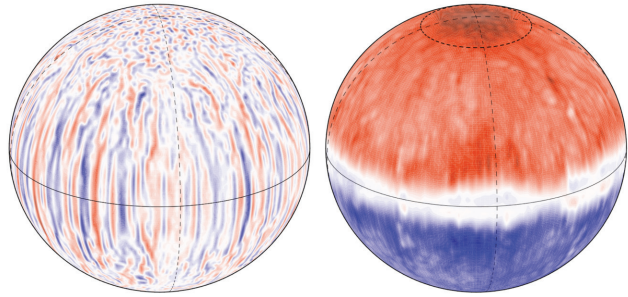


**Figure 2:** Contour plots for the radial velocity at  $r = 0.8r_o$ , where  $r_o$  is the outer radius (left panel), and the radial magnetic field at  $r = r_o$  (right panel). The plots show longitudes spaced  $90^\circ$  apart and the equator. The thick dashed line in the magnetic field plot is the latitude at which the tangent cylinder (imaginary cylinder that circumscribes the inner core and parallel to the rotation axis) cuts the core surface ( $\approx 70^\circ$ ). The figures represent a dynamo model at  $E = 1.5 \times 10^{-6}$ ,  $Ra \approx 50 \times Ra_c$ ,  $Pr = 1$  &  $q = Pm = 0.1$ .

Snapshots of the flow and field produced in a dynamo simulation are given in figure 2. The long-time columnar structure of convection has origins in the Taylor-Proudman theorem<sup>25,26</sup> for a rotating fluid; the number of columns increases with decreasing Ekman number, as predicted by linear theory<sup>27</sup>. Although columns are the enduring feature of convection in rotating dynamos, recent studies<sup>28</sup> indicate that the columns may be the long-time manifestation of damped fast Magneto-Coriolis (MC) waves that propagate along the rotation axis. The large-scale axial dipole structure (figure 2, right panel) is a dominant feature of the radial magnetic field generated in rapidly rotating dynamo models.

### The Axial Dipole and Polarity Reversals

Most planetary dynamos are approximately axial dipoles, the exceptions being Uranus and Neptune, whose physical properties are not well understood. Studies of convection-driven dynamo models show that different polarities of the magnetic field may be generated, such as the axial dipole, quadrupole<sup>29</sup> and even the equatorial dipole<sup>30</sup>, that is, a dipolar field with its axis on the equatorial plane. However, the axial dipole forms in a wide range of the parameter space where the nonlinear inertial term is negligible in the equation of motion<sup>31</sup>. Recent simulations of strongly driven and rapidly rotating dynamos<sup>32</sup> indicate that the axial dipole would be favored in the Earth-like parameter regime of low Ekman number  $E$  and low magnetic Prandtl number  $Pm$ . However, columns parallel to the rotation axis by themselves do not necessarily lead to an axial dipole field. Rotating kinematic dynamo

models at low Ekman number and low magnetic Prandtl number<sup>33</sup> favour quadrupolar modes over dipolar modes, even though the z-velocity has the same equatorial symmetry as that for convection-driven flow in rotating spherical geometry. Sreenivasan and Jones<sup>34</sup> showed that an axial dipole gives rise to enhanced velocity gradients  $\partial u_z / \partial z$  above and below the equator, and the in-phase relation between the velocity and vorticity (curl of the velocity) produces enhanced kinetic helicity compared with that found with quadrupolar fields or in non-magnetic convection. Because helicity is thought to be an important ingredient for dynamo action, an axial dipole can form from a seed magnetic field of mixed polarity. Although the mechanism outlined above may only operate at certain length scales in the dynamo, it helps explain why the axial dipole is preferred in nonlinear dynamos, but fails to pick up strength in kinematic dynamos at the same parameters. Given that strong convective motions negate the helicity generated by the field, any explanation for dipole collapse, including polarity reversals, must originate from an explanation for the selection of the dipole in rotating dynamos.

Geomagnetic reversals are perhaps the most interesting phenomena in geophysics. Magnetic records from ancient volcanic rock and sea-bed sediments are our main source of information on reversals. The average reversal frequency in the last 20 Ma was about 5 every Ma, but the last reversal, named after Matuyama and Brunhes, had occurred

0.78 Ma ago. During reversals, the axial dipole moment can decrease by a factor of 5 compared to its time-averaged value. The dipole moment begins its decline 60–80 kyr before a reversal and recovers rapidly (within a few thousand years) after the dipole transition. There have been long periods without recorded reversals, notably the Cretaceous Normal Superchron of 118–83 Ma and the Kiaman Reverse Superchron of 312–262 Ma. Excursions, the periods during which the dipole axis deviates considerably from the pole before returning to its original state, have been frequent in Earth's history. As reversals and excursions likely occur from similar convection states of the core<sup>35</sup>, it is possible that the geodynamo operates for long periods in a narrow transition zone that lies between dipolar and chaotic field configurations. In between, however, the dynamo might pass through relatively quiet periods that make the superchrons.

The first polarity reversal in a geodynamo model was obtained by Glatzmaier & Roberts<sup>36</sup>. Since then several strongly-driven dynamos have reported spontaneous polarity reversals<sup>37,38,39</sup>, some resembling paleomagnetic reversals. Most reversing dynamos have operated in a high Ekman number ( $E \gtrsim 10^{-4}$ ) regime, which has been justified on grounds of suitability for long simulations. A high Ekman number is a natural choice for studying reversals as a strong convective state is obtained for moderate Rayleigh numbers.

The progression from a stable, dipole state to a reversing state may be obtained by gradually increasing the driving force (buoyancy) in a convection-driven dynamo model. Figure 3 shows the magnetic colatitude  $\theta$  (angle made by the field with respect to the vertical axis) at the core–mantle boundary for three convective states of progressively increasing strength. The non-reversing axial dipole component is dominant for  $Ra_M = 810$ , whereas for  $Ra_M = 990$ , excursions and reversals of the dipole are present. The case  $Ra_M = 1350$  is a chaotic, multipolar dynamo. The axial dipole component of  $\mathbf{B}$  is shown in figure 4 for three snapshots in time at the start, during and at the end of a polarity reversal. The reversal period is  $\approx 0.1$  magnetic diffusion time, consistent with the estimate of a few thousand years for the core<sup>40</sup>.

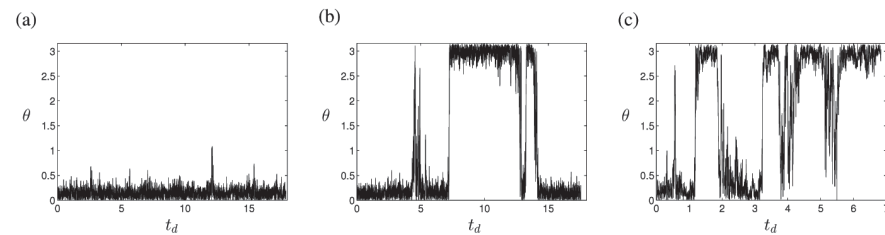


**Figure 3:** Dipole colatitude versus magnetic diffusion time for geodynamo simulations at three states of convection, given by the modified Rayleigh numbers (a)  $Ra_M = 810$ , (b)  $Ra_M = 990$  and (c)  $Ra_M = 1350$ . (Figure taken from Sreenivasan, Sahoo & Dharma, Geophys. J. Int. (2014), 199, 1698–1708).

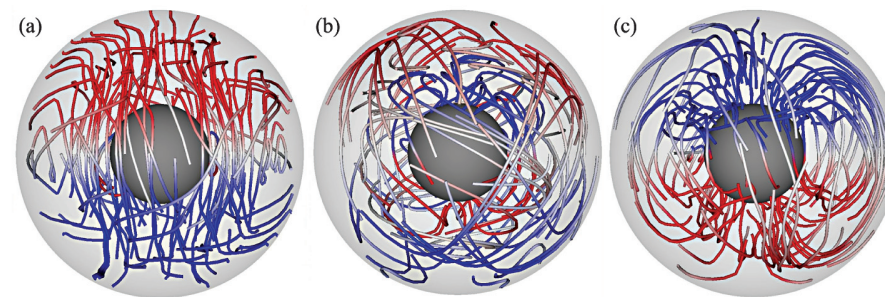


**Figure 4:** Streamlines of the axial dipole component of the magnetic field vector shown at three different snapshots in time during a polarity reversal at the modified Rayleigh number  $Ra_M = 990$ . The time elapsed between the first and third snapshots is approximately 0.1 magnetic diffusion time. (Figure taken from Sreenivasan, Sahoo & Dharma, Geophys. J. Int. (2014), 199, 1698–1708).

## Conclusion

Paleomagnetic records indicate that the Earth's magnetic field is ancient. Since permanent magnetization cannot be a source for this field, dynamo action within the Earth's fluid core is widely accepted as the mechanism for field generation. Although convection, both thermal and compositional, is believed to be the main driving mechanism for core motion, precession of the Earth's rotation axis and tidal deformation of the core–mantle boundary have also been considered<sup>41</sup>. Geodynamo models have improved our understanding of the physical processes within the core that sustain the planet's dipole-dominated magnetic field. Deviations from the axisymmetric dipole, such as the high-latitude flux concentrations beneath Canada and Siberia<sup>42</sup> and regions of weak or reversed polar flux<sup>43</sup>, have been investigated by incorporating lower-mantle heat flux anomalies in dynamo models, as well as by looking at tangent cylinder phenomena. As dynamo models are unable to reach the Ekman number of the Earth, the effect of small length scales on the dynamo process may be understood only through simplified models of core turbulence. Furthermore, as small-scale MHD turbulence in the core is likely in a state of perpetual damped wave motion<sup>28</sup>, their role in dynamo energy transport and secular variation of the field may be far more important than previously envisaged. Recent ideas of enhanced thermal conductivity of liquid iron in the core favour the existence of stably stratified regions, whose effect on the dynamo process needs to be known. Laboratory experiments with liquid metals are useful because they reach the geophysically relevant regime of low magnetic Prandtl number, otherwise impossible in present day simulations.

## References

1. E. Halley, *Philosophical Transactions* **13**, 208 (1683).
2. E. Halley, *Philosophical Transactions* **16**, 563 (1692).
3. H. K. Moffatt, *Magnetic field generation in electrically conducting fluids* (Cambridge University Press, 1978).
4. J. Larmor, *Brit. Assn. Adv. Sci. Rep.*, 159 (1919).
5. R. D. Oldham, *Quaternary J. Geol. Soc.* **62**, 456 (1906).
6. B. Gutenberg, *Physika Zeitschrift* **14**, 1217 (1913).
7. J. A. Tarduno, R. D. Cottrell, M. K. Watkeys, A. Hofmann, P. V. Doubrovine, E. E. Mamajek, D. Liu, D. G. Sibeck, L. P. Neukirch, and Y. Usui, *Science* **327**, 1238 (2010).
8. T. Nakagawa and P. J. Tackley, *Geophys. Res. Lett.* **40**, 2652 (2013).
9. C. A. Jones, in *Core Dynamics*, Treatise on Geophysics, Vol. 8, edited by P. Olson (Elsevier B. V., 2015) pp. 115–159.
10. U. R. Christensen and J. Wicht, in *Core Dynamics*, Treatise on Geophysics, Vol. 8, edited by P. Olson (Elsevier B. V., 2015) pp. 245–277.
11. W. M. Elsasser, *Phys. Rev.* **69**, 106 (1946).
12. E. Bullard and H. Gellman, *Phil. Trans. R. Soc. A* **247**, 213 (1954).
13. E. N. Parker, *Astrophys. J.* **122**, 293 (1955).
14. F. Steenbeck, M. and Krause and K. H. Rädler, *Z. Naturforsch A* **21**, 369 (1966).
15. B. Sreenivasan, *Curr. Sci.* **99**, 1739 (2010).
16. S. Kumar and P. H. Roberts, *Proc. R. Soc. Lond. A* **344**, 235 (1975).
17. M. L. Dudley and R. W. James, *Proc. R. Soc. Lond. A* **425**, 407 (1989).
18. P. A. Davidson, *An Introduction to Magnetohydrodynamics* (Cambridge University Press, 2001).
19. M. Kono and P. H. Roberts, *Rev. Geophys.* **40**, 1013 (2002).
20. T. C. Clune, J. R. Elliot, M. S. Miesch, J. Toomre, and G. A. Glatzmaier, *Parallel Computing* **25**, 361 (1999).
21. A. P. Willis, B. Sreenivasan, and D. Gubbins, *Phys. Earth Planet. Inter.* **165**, 83 (2007).
22. D. Gubbins, *Phys. Earth Planet. Int.* **128**, 3 (2001).
23. P. Olson, in *Earth's Core and Lower Mantle, The Fluid Mechanics of Astrophysics and Geophysics*, Vol. 11, edited by C. A. Jones, A. M. Soward, and K. Zhang (Taylor & Francis, London & New York, 2003) pp. 1–38.
24. A. P. Anufriev, C. A. Jones, and A. M. Soward, *Phys. Earth Planet. Int.* **152**, 163 (2005).
25. J. Proudman, *Proc. R. Soc. Lond. A* **92**, 408 (1916).
26. G. I. Taylor, *Proc. R. Soc. Lond. A* **102**, 180 (1923).
27. S. Chandrasekhar, *Hydrodynamic and hydromagnetic stability* (Clarendon Press, Oxford, 1961).
28. B. Sreenivasan and G. Narasimhan, *J. Fluid Mech.* **828**, 867 (2017).
29. E. Grote, F. H. Busse, and A. Tilgner, *Phys. Earth Planet. Inter.* **117**, 259 (2000).
30. N. Ishihara and S. Kida, *Fluid Dyn. Res.* **31**, 253 (2002).
31. B. Sreenivasan and C. A. Jones, *Geophys. J. Int.* **164**, 467 (2006).
32. N. Schaeffer, D. Jault, H.-C. Nataf, and A. Fournier, *Geophys. J. Int.* **211**, 1 (2017).
33. N. Schaeffer and P. Cardin, *Earth Planet. Sci. Lett.* **245**, 595 (2006).
34. B. Sreenivasan and C. A. Jones, *J. Fluid Mech.* **103**, 1 (2011).
35. D. Gubbins, *Geophys. J. Int.* **137**, 1 (1999).
36. G. A. Glatzmaier and P. H. Roberts, *Nature* **377**, 203 (1995).
37. C. Kutzner and U. R. Christensen, *Phys. Earth Planet. Int.* **131**, 29 (2002).
38. J. Wicht and P. Olson, *Geochem. Geophys. Geosyst.* **5**, Q03H10 (2004).
39. F. Takahashi, M. Matsushima, and Y. Honkura, *Earth Planets Space* **59**, 665 (2007).
40. R. T. Merrill and P. L. McFadden, *Rev. Geophys.* **37**, 201 (1999).
41. A. Tilgner, in *Core Dynamics*, Treatise on Geophysics, Vol. 8, edited by P. Olson (Elsevier B. V., 2015) pp. 183–212.
42. D. Gubbins, A. P. Willis, and B. Sreenivasan, *Phys. Earth Planet. Inter.* **162**, 256 (2007).
43. B. Sreenivasan and C. A. Jones, *Geophys. Astrophys. Fluid Dyn.* **100**, 319 (2006).